

ROMAN Z. MORAWSKI, CEZARY NIEDZIŃSKI

Warsaw University of Technology,
Faculty of Electronics and Information Technology,
Institute of Radioelectronics
Warsaw, Poland
e-mail: r.morawski@ire.pw.edu.pl

APPLICATION OF A BAYESIAN ESTIMATOR FOR IDENTIFICATION OF EDIBLE OILS ON THE BASIS OF SPECTROPHOTOMETRIC DATA

Spectrophotometric analysis of oil mixtures, containing olive oil, is the subject of this paper. Its objective is to compare a new Bayesian estimator with the constrained least-squares estimator, when applied for estimation of concentrations of components of edible oil mixtures, and to assess its applicability for solving problems of industrial monitoring. The comparison is based on the use of semi-synthetic NIR spectrophotometric data and criteria related to measurement uncertainty.

Keywords: NIR spectrophotometry, chemometrics, Bayesian estimation, olive oil

1. INTRODUCTION

The quality and purity of olive oil, extensively used in food industry, is of significant commercial importance. According to the EU regulations in force since 2002, a manufacturer of products based on or containing olive oil, must either indicate the share of olive oil (and other oil components) in the total weight of the product or the percentage of the total fat. That is why an increased interest in the methods for oil mixtures analysis has been observed for the last five years. Near-infrared (NIR) spectrophotometry, when combined with sophisticated procedures for spectrophotometric data processing, seems to be the most promising tool for such applications, as suggested in many recent publications [1-5]. In general, NIR spectrophotometry is of particular usefulness for food analysis because spectra of organic samples comprise broad bands arising from overlapping absorption peaks corresponding to C-H, O-H and N-H chemical bonds. The main advantage of NIR spectrophotometry, when applied to off-laboratory analysis of food, is its simplicity and speed: usually no sample preparation is necessary and the time of analysis is not greater than 1 minute. Another advantage of NIR spectrophotometry is that it allows several constituents to be identified concurrently. Finally, the relatively weak absorption due to water enables one to analyze high-moisture food products and ingredients.

Off-laboratory applications of NIR spectrophotometry in food analysis may be roughly subdivided into two classes: fraud detection and monitoring of manufacturing processes. This paper is devoted to an instance of the latter one, viz. to the monitoring of edible oils mixing. The monitoring-type problems have two specific features:

- a monitoring instrument is repeating – over a long period of time – the same measurement function, i.e. it is measuring the same quantities, in the same range, with the same uncertainty;

- the ranges of their variation are relatively narrow and known a priori.

Both those features may be used for improving the performance of NIR analysis without significant costs – by the deliberate use of them in the procedures for NIR data processing. The Bayesian framework seems to be most appropriate for the development of such procedures because historical data, acquired during a sufficiently long monitoring run, contain very reliable a priori information on measurands and may be used for constructing corresponding probability density functions. This paper is devoted to the comparison of the Bayesian method, developed for Vis-spectrometric applications in a recently-defended Ph.D. thesis [6], with a constrained least-squares method, when applied for quantitative determination of ternary oil mixtures on the basis of the data representative of their NIR spectra. Both compared methods are nonlinear because they incorporate non-trivial constraints of the space of feasible solutions, thus - potentially predisposed to provide lower uncertainty of estimation than the linear method of ordinary least squares.

The paper is organized as follows. First, in Section 2, a mathematical model of spectrophotometric data, underlying the Bayesian method to be studied, is briefly described. Next, in Sections 3 and 4, the Bayesian method itself and its implementation are presented using a mathematical model of the data introduced in Section 2. Finally, in Sections 5-6, the methodology of study and the results of study are presented. The conclusions, provided in Section 7, are mainly concentrated on the metrological properties of the studied Bayesian method and its practical utility for solving the problem of monitoring oil mixing processes.

The following general rules are consistently used throughout the paper for generation of mathematical symbols:

- x, y, \dots are real-valued scalar variables;

- $\mathbf{x}, \mathbf{y}, \dots$ are vectors of real-valued variables;

- $\mathbf{X}, \mathbf{Y}, \dots$ are matrices of real-valued variables;

- \hat{x}, \hat{y}, \dots are exact values of the variables x, y, \dots ;

- \hat{x}, \hat{y}, \dots are estimated values of the variables x, y, \dots ;

- $\hat{\mathbf{x}}, \hat{\mathbf{y}}, \dots$ are estimated values of the vectors $\mathbf{x}, \mathbf{y}, \dots$;

- $\tilde{\mathbf{x}}, \tilde{\mathbf{y}}, \dots$ are noisy versions of the vectors $\mathbf{x}, \mathbf{y}, \dots$;

- $\underline{x}, \underline{y}, \dots$ are random variables whose realizations are denoted with x, y, \dots ;

- $\underline{\mathbf{x}}, \underline{\mathbf{y}}, \dots$ are random vectors whose realizations are denoted with $\mathbf{x}, \mathbf{y}, \dots$;

All mathematical symbols, used in the paper, are alphabetically listed in the Appendix.

2. MATHEMATICAL MODEL OF SPECTROPHOTOMETRIC DATA

A spectrophotometer to be used for determination of oil mixtures consists of a sampling block (comprising a light source and a sample holder), a spectrophotometric transducer (ST) and a digital interface enabling communication with a computing means (i.e. a regular computer or a microprocessor or a digital signal processor) loaded with a corresponding piece of software (firmware). The ST is converting an optical signal into a digital signal - the data representative of the spectrum of the input optical signal. Numerical processing of those data by computing means comprises all the operations necessary for transforming “meaningless” digital codes into “meaningful” representation of the spectrum – in the transmittance domain or in the absorbance domain - with an uncertainty not exceeding some predefined limits. It may also provide some results of spectrum interpretation, e.g. the estimates of magnitudes and positions of absorption peaks. In the majority of spectrophotometers available on the today’s market, the ST is based on a grating-type dispersive element followed by an array of photodiodes (a photodetector), converting optical into electrical signals, and an analogue-to-digital converter. This solution implies the discretisation of the wavelength axis that may be defined by a sequence of wavelength values $\{\lambda_n\}$ such that:

$$\lambda_{\min} = \lambda_1 < \lambda_2 < \dots < \lambda_{N-1} < \lambda_N = \lambda_{\max} \quad (1)$$

where N is the number of data provided at the ST output, i.e. the number of photodiodes in the photodetector.

The intensity data, provided by an ST, may be modelled using a white-box approach, a black-box approach, or a grey-box approach combining some advantages of white-box and black-box approaches [7]. 80 years of experience behind modelling of spectrophotometric data seems to support the conclusion that the approximation power of a superposition of a linear integral operator with a nonlinear algebraic operator (the so-called Wiener operator) is sufficient for adequate modelling of the relationship between the intensity spectrum $x(\lambda)$ and the corresponding raw data $\tilde{\mathbf{y}} = [\tilde{y}_1 \dots \tilde{y}_N]^T$. Let the variable \hat{y}_n denote the mathematical model of the “noise-free” version of the datum \tilde{y}_n . Then this operator may be given the form:

$$\hat{y}_n = F \left(\int_{-\infty}^{+\infty} g_n(\lambda_n - \lambda) x(\lambda) d\lambda; \boldsymbol{\alpha}_n \right) \quad \text{for } n = 1, \dots, N \quad (2)$$

where:

- $g_n(\lambda)$ is the response of the ST, measured at the output of the n th photodiode, to a tunable monochromator producing an optical signal whose spectrum is close to $x(\lambda) \cong \delta(\lambda - l)$ where l is sweeping the wavelength range $[\lambda_{\min}, \lambda_{\max}]$;

- $F(\bullet; \alpha_n)$ is an *a priori* known function (e.g. an algebraic polynomial or a cubic spline) whose parameters, organised in a vector α_n , have to be determined during the ST calibration.

The reasoning presented for the intensity-domain data may be applied to the transmittance-domain data. As a rule, due to the compensation of some irregularities by the division of corresponding intensity data, the function $F(\bullet; \alpha$ can be less complex in this case, and the variability of α and $g_n(\lambda)$ along the wavelength axis – less important. Consequently, in many cases this variability may be ignored and the corresponding model of the transmittance-domain data can be simplified by fixing: $\alpha_n \equiv \alpha$ and $g_n(\lambda)$ for $n = 1, \dots, N$. This analysis justifies the use of the following mathematical model of the relationship between the transmittance spectrum $x^{Tr}(\lambda)$ and the corresponding data $\tilde{\mathbf{y}}^{Tr} = [\tilde{y}_1^{Tr} \dots \tilde{y}_N^{Tr}]^T$:

$$\tilde{y}_n^{Tr} = \int_{-\infty}^{+\infty} g(\lambda_n - \lambda) x^{Tr}(\lambda) d\lambda + \eta_n \quad \text{for } n = 1, \dots, N \quad (3)$$

where the additive residuals η_n represent the total uncertainty of data modelling.

For the purpose of modelling the dependence of the data on concentrations, one may use the Lambert-Beer laws of absorption to relate $x^{Tr}(\lambda)$ in Eq.(3) to the vector of concentrations $\mathbf{c} = [c_1 \dots c_J]^T$:

- the absorbance of a solution of a single component is proportional to its concentration;
- the absorbance spectrum of a multicomponent solution:

$$x^{Ab}(\lambda) = -\log_{10} [x^{Tr}(\lambda)] \quad (4)$$

equals the linear combination:

$$x^{Ab}(\lambda) = c_1 x_1^{Ab}(\lambda) + \dots + c_J x_J^{Ab}(\lambda) \quad (5)$$

of the normalized absorbance spectra of the components $x_1^{Ab}(\lambda), \dots, x_J^{Ab}(\lambda)$.

Eq.(3), Eq.(4) and Eq.(5) should undergo discretisation to become a useful basis for the development of numerical methods for estimation of concentrations. Thus, Eq.(3) is replaced with:

$$\tilde{\mathbf{y}}^{Tr} = \mathbf{G} \cdot \mathbf{x}^{Tr} + \boldsymbol{\eta} \quad (6)$$

where:

$$\boldsymbol{\eta} = [\eta_1 \dots \eta_N]^T \quad (7)$$

$$\mathbf{x}^{Tr} = [x^{Tr}(\lambda'_1) \dots x^{Tr}(\lambda'_M)]^T \quad (8)$$

$$\lambda'_m = \lambda_{\min} + (m - 1) \frac{\lambda_{\max} - \lambda_{\min}}{M - 1} \quad \text{for } m = 1, \dots, M \quad (9)$$

and \mathbf{G} is an $N \times M$ matrix whose values depend on the values of the function $g(\lambda)$ and on the chosen method of numerical integration. The discretisation of Eq.(4) and Eq.(5), consistent with Eq (6), yields:

$$\mathbf{x}^{Ab} = \left[-\log_{10} \left(x^{Tr}(\lambda'_1) \right) \dots -\log_{10} \left(x^{Tr}(\lambda'_M) \right) \right]^T \quad (10)$$

$$\mathbf{x}^{Ab} = c_1 \mathbf{x}_1^{Ab} + \dots + c_J \mathbf{x}_J^{Ab} = \mathbf{X}^{Ab} \mathbf{c} \quad (11)$$

where:

$$\mathbf{x}_j^{Ab} = \left[x_j^{Ab}(\lambda'_1) \dots x_j^{Ab}(\lambda'_M) \right]^T \quad \text{for } j = 1, \dots, J \quad (12)$$

$$\mathbf{X}^{Ab} = \left[\mathbf{x}_1^{Ab} \dots \mathbf{x}_J^{Ab} \right] \quad (13)$$

The up-to-now developed model of the relationship $\mathbf{c} \rightarrow \tilde{\mathbf{y}}^{Tr}$ characterizes this relationship for one particular pair of \mathbf{c} and $\tilde{\mathbf{y}}^{Tr}$. It should be generalized to the populations of possible vectors \mathbf{c} and $\tilde{\mathbf{y}}^{Tr}$ to make possible the use of a probabilistic framework. This can be achieved by introducing random vectors (denoted hereinafter with underlined symbols) for modelling unknowns. The randomization of the vector $\boldsymbol{\eta}$, modelling uncertainty, yields:

$$\underline{\tilde{\mathbf{y}}}^{Tr} = \mathbf{G} \cdot \mathbf{x}^{Tr} + \underline{\boldsymbol{\eta}} \quad (14)$$

where $\underline{\boldsymbol{\eta}} = \left[\underline{\eta}_1 \dots \underline{\eta}_N \right]^T$. The model of the relationship between concentrations and absorbance spectrum, corresponding to Eq.(11) takes on the form:

$$\underline{\mathbf{x}}^{Ab} = \mathbf{X}^{Ab} \underline{\mathbf{c}} + \underline{\boldsymbol{\varepsilon}} \quad (15)$$

where

$\underline{\mathbf{c}} = \left[\underline{c}_1 \dots \underline{c}_J \right]^T$ is the random vector of the concentrations to be estimated, $\underline{\boldsymbol{\varepsilon}} = \left[\underline{\varepsilon}_1 \dots \underline{\varepsilon}_M \right]^T$ is the random vector containing samples of the residual spectrum representative of unexpected or neglected components, and CAT is the operator of absorbance-to-transmittance conversion:

$$\underline{\mathbf{x}}^{Tr} = \left[\underline{x}_1^{Tr} \dots \underline{x}_M^{Tr} \right]^T = \text{CAT} \left[\underline{\mathbf{x}}^{Ab} \right] = \left[10^{-\underline{x}_1^{Ab}} \dots 10^{-\underline{x}_M^{Ab}} \right]^T \quad (16)$$

The substitution of Eq.(15) to Eq.(16) and then of Eq.(16) to Eq.(14) yields a compact-form, discretised and randomized model of the data underlying the Bayesian method described in the next section:

$$\underline{\tilde{\mathbf{y}}}^{Tr} = \mathbf{G} \cdot \text{CAT} \left[\mathbf{X}^{Ab} \underline{\mathbf{c}} + \underline{\boldsymbol{\varepsilon}} \right] + \underline{\boldsymbol{\eta}} \quad (17)$$

It should be noted that this model, developed for a grating-based ST, is also valid for other types of STs.

3. FORMULATION OF THE RESEARCH PROBLEM AND PROPOSED SOLUTION

The research problem to be solved can be now formulated as follows: given the matrix \mathbf{X}^{Ab} (containing discretised spectra of selected edible oils), the matrix \mathbf{G} (representative of the apparatus function of the spectrophotometer), and some a priori information on the probabilistic properties of the random vectors $\boldsymbol{\eta}$, $\boldsymbol{\varepsilon}$ and c – estimate the vector of concentrations \mathbf{c} , using the spectrophotometric data $\tilde{\mathbf{y}}^{Tr}$ representative of the oil mixture to be analyzed.

A most natural tool for relating the uncertainty of the raw data used for measurand estimation and uncertainty of the a priori information on the measurand to the final result of measurement is the Bayes theorem [8]. Known for two centuries, the Bayesian approach became a “popular” tool for processing measurement data only ten years ago, when available computational power of PCs made it implementable. It follows from the Bayes’ theorem that the probability density function, representative of the a posteriori probability of the final result of measurement conditional on the data (the so-called posterior) is proportional to the product of:

- a probability density function representative of all the a priori information on the model of the data and on the uncertainty of the raw measurement data;
- a probability density function representative of all the available a priori information on the measurand.

Thus, the posterior contains all the available a priori information that may be used for solving the problem of measurand estimation. The most common approach consists in maximization of the posterior with respect to the measurand. In practice, however, many simplified approaches have been developed to avoid or overcome difficulties related to the numerical complexity intrinsic of this approach when applied to such a generic optimization problem.

The Bayesian method for the estimation of c using a realization $\tilde{\mathbf{y}}^{Tr}$ of $\tilde{\mathbf{y}}^{Tr}$, developed and studied in the source Ph.D. thesis [6], is derived from the following Bayes’ formula:

$$f_{\underline{\mathbf{c}}|\tilde{\mathbf{y}}^{Tr}}(\mathbf{c}|\tilde{\mathbf{y}}^{Tr}) = \frac{f_{\tilde{\mathbf{y}}^{Tr}|\mathbf{c}}(\tilde{\mathbf{y}}^{Tr}|\mathbf{c}) f_{\underline{\mathbf{c}}}(\mathbf{c})}{f_{\tilde{\mathbf{y}}^{Tr}}(\tilde{\mathbf{y}}^{Tr})} \quad (18)$$

where $f_{\underline{\mathbf{c}}}(\mathbf{c})$ is the a priori probability density function for $\tilde{\mathbf{y}}^{Tr}$; $f_{\tilde{\mathbf{y}}^{Tr}|\mathbf{c}}(\tilde{\mathbf{y}}^{Tr}|\mathbf{c})$ is the a priori probability density function for $\tilde{\mathbf{Y}}^{Tr}$; $f_{\underline{\mathbf{c}}|\tilde{\mathbf{y}}^{Tr}}(\mathbf{c}|\tilde{\mathbf{y}}^{Tr})$ is the a posteriori probability

density function for $\underline{\mathbf{c}}$ conditional on $\tilde{\mathbf{y}}^{Tr}$; and $f_{\tilde{\mathbf{y}}^{Tr}|\mathbf{c}}(\tilde{\mathbf{y}}^{Tr}|\mathbf{c})$ is the probability density function for $\tilde{\mathbf{y}}^{Tr}$ conditional on \mathbf{c} . In general, the Bayesian estimation of concentrations may be based on the mean value or median or maximum value of the function defined by Eq.(18) In the method of estimation to be studied hereinafter, the following approach is used:

$$\hat{\mathbf{c}} = \arg_{\mathbf{c}} \sup \left\{ f_{\underline{\mathbf{c}}|\tilde{\mathbf{y}}^{Tr}}(\mathbf{c}|\tilde{\mathbf{y}}^{Tr}) \mid \mathbf{c} \in \mathbf{C} \right\} = \arg_{\mathbf{c}} \sup \left\{ f_{\tilde{\mathbf{y}}^{Tr}|\mathbf{c}}(\tilde{\mathbf{y}}^{Tr}|\mathbf{c}) f_{\underline{\mathbf{c}}}(\mathbf{c}) \mid \mathbf{c} \in \mathbf{C} \right\} \quad (19)$$

where: $\mathbf{C} = \{\mathbf{c} \mid c_1, \dots, c_J \geq 0; c_1 + \dots + c_J \leq 1\}$. The omission of the function $f_{\tilde{\mathbf{y}}^{Tr}}(\tilde{\mathbf{y}}^{Tr})$ in this formula is justified by its independence of \mathbf{c} .

4. IMPLEMENTATION OF THE PROPOSED SOLUTION

First, the Bayesian method, described in the previous section, has been adapted to the condition $c_1 + \dots + c_J = 1$ satisfied by any oil mixture to be analysed. Due to the equality implied by this condition:

$$x^{Ab}(\lambda) = \sum_{j=1}^J c_j x_j^{Ab}(\lambda) = \sum_{j=1}^{J-1} c_j x_j^{Ab}(\lambda) + \left(1 - \sum_{j=1}^{J-1} c_j\right) x_J^{Ab}(\lambda) = \sum_{j=1}^{J-1} c_j [x_j^{Ab}(\lambda) - x_J^{Ab}(\lambda)] + x_J^{Ab}(\lambda) \quad (20)$$

the estimated vector of concentrations has been reduced to $\mathbf{c} = [c_1 c_2 \dots c_{J-1}]^T$, and the statistical independence of the corresponding random variables $\underline{c}_1, \underline{c}_2, \dots, \underline{c}_{J-1}$ has been assumed. The model of the data has been, consequently, modified accordingly:

$$\tilde{\mathbf{y}}^{Tr} = \mathbf{G} \cdot \text{CAT} \left[\mathbf{X}^{Ab} \underline{\mathbf{c}} + \mathbf{x}_J^{Ab} + \underline{\boldsymbol{\varepsilon}} \right] + \underline{\boldsymbol{\eta}} \quad (21)$$

where:

$$\mathbf{X}^{Ab} = \left[\begin{array}{cccc} \mathbf{x}_1^{Ab} - \mathbf{x}_J^{Ab} & \mathbf{x}_2^{Ab} - \mathbf{x}_J^{Ab} & \dots & \mathbf{x}_{J-1}^{Ab} - \mathbf{x}_J^{Ab} \end{array} \right] \quad (22)$$

Next, taking into account that the uncontrollable components in food products to be analyzed must be at the trace level, it has been assumed that the norms of the realizations of the random vector $\underline{\boldsymbol{\varepsilon}}$ are small enough to justify the following simplification:

$$f_{\tilde{\mathbf{y}}^{Tr}|\mathbf{c}}(\tilde{\mathbf{y}}^{Tr}|\mathbf{c}) = \mathbb{E} \left[f(\underline{\boldsymbol{\varepsilon}}) \right] = f_{\underline{\boldsymbol{\eta}}} \left\{ \tilde{\mathbf{y}}^{Tr} - \mathbf{G} \cdot \text{CAT} \left[\mathbf{X}^{Ab} \mathbf{c} + \mathbf{x}_J^{Ab} + \underline{\boldsymbol{\mu}}_{\boldsymbol{\varepsilon}} \right] \right\} \quad \text{with } \underline{\boldsymbol{\mu}}_{\boldsymbol{\varepsilon}} = \mathbb{E} \left[\underline{\boldsymbol{\varepsilon}} \right] \quad (23)$$

$$\hat{\mathbf{c}} = \arg_{\mathbf{c}} \sup \left\{ f_{\underline{\mathbf{c}}|\underline{\mathbf{y}}^{Tr}}(\mathbf{c}|\underline{\mathbf{y}}^{Tr}) \mid \mathbf{c} \in \mathbf{C} \right\} = \arg_{\mathbf{c}} \sup \left\{ f_{\underline{\mathbf{y}}^{Tr}|\mathbf{c}}(\underline{\mathbf{y}}^{Tr}|\mathbf{c}) f_{\underline{\mathbf{c}}}(\mathbf{c}) \mid \mathbf{c} \in \mathbf{C} \right\} \quad (24)$$

where:

$$\mathbf{C} = \{\mathbf{c} \mid 0 \leq c_1, \dots, c_{J-1} \leq 1\} \quad (25)$$

Finally, the Bayesian method, adapted to the target application, has been implemented under an assumption that the components of the vector $\underline{\boldsymbol{\eta}}$ are statistically independent and that its distribution is Gaussian, *i.e.*:

$$f_{\underline{\boldsymbol{\eta}}}(\boldsymbol{\eta}) = \frac{1}{\sqrt{(2\pi\sigma_{\eta}^2)^N}} \exp\left(-\frac{\boldsymbol{\eta}^T \boldsymbol{\eta}}{2\sigma_{\eta}^2}\right) \quad (26)$$

where σ_{η}^2 is the variance of the elements of the vector $\underline{\boldsymbol{\eta}}$. Additionally, unlike in the source thesis [6], it has been assumed that the components of the vector \mathbf{c} are statistically independent and its a priori probability density function has the form:

$$f_{\underline{\mathbf{c}}}(\mathbf{c}) = A \cdot \exp\left(-\frac{[\mathbf{v}(\mathbf{c})]^T \cdot \mathbf{v}(\mathbf{c})}{2\sigma_v^2}\right) \quad (27)$$

where A is a normalization factor, and $\mathbf{v}(\mathbf{c})$ is a $(J - 1)$ -dimensional vector whose elements are defined by the following transformation of the finite interval $[0, 1]$ into the infinite interval $(-\infty, +\infty)$:

$$v_j(\mathbf{c}) \equiv \frac{c_j - \hat{c}_j}{c_j(1 - c_j)} \quad \text{for } j = 1, \dots, J - 1 \quad (28)$$

with \hat{c}_j being the value of c_j for which the corresponding marginal probability density function attains maximum. It should be noted that the values of \hat{c}_j and σ_v are close to but not identical with the mean value and standard deviation of $\underline{\mathbf{c}}$, respectively; the differences are shown in Fig. 1.

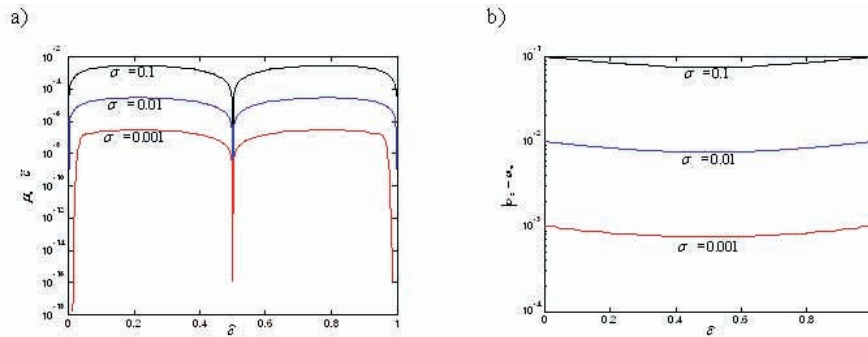


Fig. 1. The dependence on \hat{c} and σ_v of the departure of the mean value μ_c of the random variable \underline{c} from \hat{c} (a) and of the standard deviation σ_c of \underline{c} from σ_v (b).

The heuristic form of the a priori probability density function for c has been chosen due to the lack of statistical data representative of a particular manufacturing process to be monitored. Once such an application is selected, the distribution defined by Eq.(27) should be replaced with an empirical distribution of c obtained on the basis of historical data characterizing this application. The assumed a priori probability density function for η is a good choice for the majority of measurement situations where the total measurement uncertainty is the combined effect of many factors of comparable magnitude: if one of them is dominating (e.g. the error of analogue-to-digital conversion), then the use of the distribution characterizing this factor may be justified (e.g. a uniform distribution).

The Bayesian method adapted to the target application, called BM hereinafter, has been implemented using MATLAB ver. 7.5, supported by a MATLAB-compatible software package of global optimization TOMLAB ver. 6.0 [9]. The estimation of concentrations according to Eq.(24) has been implemented in MATLAB via the minimization of the following goal function: function value = FUN(\mathbf{c})

$$value = \frac{[\mathbf{v}(\mathbf{c})]^T \cdot \mathbf{v}(\mathbf{c})}{2\sigma_v^2} + \frac{1}{\sigma_\eta^2} \left\| \tilde{\mathbf{y}}^{Tr} - \mathbf{G} \cdot \text{CAT}(\mathbf{X}^{Ab}\mathbf{c} + \mathbf{x}_j^{Ab} + \boldsymbol{\mu}_\varepsilon) \right\|^2$$

using the TOMLAB box-bounded global optimization solver glbSolve with the lower bounds defined by the vector $\mathbf{c}^{lb} = [00]^T$ and the upper bounds defined by the vector $\mathbf{c}^{ub} = [11]^T$. The BM has been implemented according to the following scheme:

- load the vectors $\mathbf{x}_j^{Ab} = 1, \dots, J$;
- form the matrix \mathbf{X}^{Ab} according to Eq.(22)
- load the vector \mathbf{g} containing the samples of the function $g(\lambda)$;
- form a convolution matrix: $\mathbf{G} = \Delta\lambda * \text{CONVMTX}(\mathbf{g}, \text{LENGTH}(\mathbf{x}_j^{Ab}))$;

- load the raw measurement data $\tilde{\mathbf{y}}^{Tr}$ to be processed;
 - load the parameters σ_η , \hat{c}_j for $j = 1, 2$, σ_v and $\boldsymbol{\mu}_\varepsilon$;
 - set up a global programming problem parameters into an input structure *Prob*: *Prob* = *glcAssign* ('FUN', \mathbf{c}^{lb} , \mathbf{c}^{ub} , 'NameOfTheProblem')
- minimize FUN by means of *glbSolve*: *Result* = *tomRun*('glbSolve', *Prob*, 0) to find the solution:

$$\hat{\mathbf{c}} = \text{Result.x.k.}$$

5. METHODOLOGY OF INVESTIGATION

The Bayesian method for estimation of concentrations, described in Section 4, i.e. the BM, has been systematically compared with the constrained least-squares method (CLSM), defined by the formula:

$$\hat{\mathbf{c}} = \arg_{\mathbf{c}} \inf \left\{ \left\| \tilde{\mathbf{y}}^{Tr} - \mathbf{G} \cdot \text{CAT} [\mathbf{X}^{Ab} \mathbf{c} + \mathbf{x}_j^{Ab}] \right\|_2 \mid \mathbf{c} \in \mathbf{C} \right\} \quad (29)$$

where the set of admissible solutions \mathbf{C} is defined by Eq.(25).

The comparative study has been based on semi-synthetic data, generated using the high-resolution real-world data representative of corn oil ($\tilde{\mathbf{x}}_1^{Ab}$), nut oil ($\tilde{\mathbf{x}}_2^{Ab}$) and olive oil ($\tilde{\mathbf{x}}_3^{Ab}$). The sequences of those data, each containing $N = 501$ data points, covering the wavelength range from to , are shown in Fig. 1 (their closeness is a source of difficulty of the problem under study). The denoised (by means of a nonlinear smoothing filter) and baseline-corrected versions of those data – $\dot{\mathbf{x}}_1^{Ab}$, $\dot{\mathbf{x}}_2^{Ab}$ and $\dot{\mathbf{x}}_3^{Ab}$ – have been used for generation of the nine sets of high-resolution data for numerical experimentation:

$$\dot{\mathbf{x}}^{Ab} = \dot{c}_1 \dot{\mathbf{x}}_1^{Ab} + \dot{c}_2 \dot{\mathbf{x}}_2^{Ab} + \dot{c}_3 \dot{\mathbf{x}}_3^{Ab} \quad (30)$$

where:

$$\dot{c}_1 \in \{0.01, 0.05, 0.09\} \quad \dot{c}_2 \in \{0.01, 0.05, 0.09\} \quad \text{and} \quad \dot{c}_3 = 1 - \dot{c}_1 - \dot{c}_2 \quad (31)$$

are concentrations to be estimated. An exemplary spectrum $\dot{\mathbf{x}}^{Ab}$ is shown in Fig. 2.

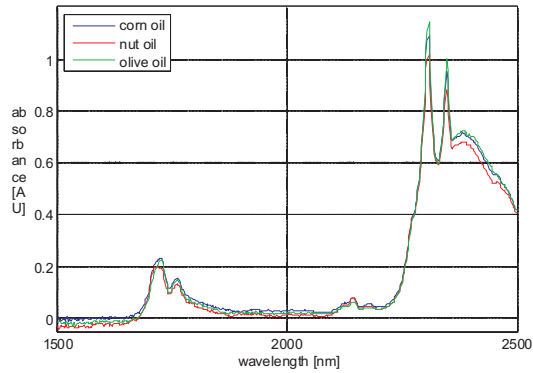


Fig. 1. The raw spectrophotometric data acquired by means of a FTIR spectrophotometer set to the resolution 1 cm^{-1} .

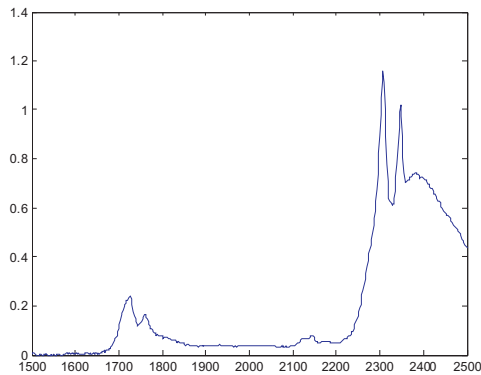


Fig. 2. The high-resolution data $\hat{\mathbf{x}}^{Ab}$ for $\hat{c}_1 = 0.01$ and $\hat{c}_2 = 0.01$.

The high-resolution data, representative of residual spectra, have been synthesized after the formula:

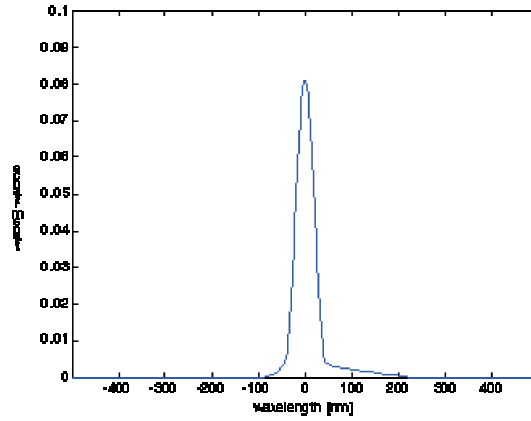
$$\underline{\varepsilon} = level \cdot (\underline{u}_1 \varepsilon_1^{Ab} + \underline{u}_2 \varepsilon_2^{Ab} + \underline{u}_3 \varepsilon_3^{Ab} + \underline{u}_4 \varepsilon_4^{Ab}) \quad (32)$$

where *level* is an indicator of the importance of the residual spectrum; u_1 , u_2 , u_3 , and u_4 are identical independent random variables following the distribution uniform in the interval $[0, 1]$; and ε_1^{Ab} , ε_2^{Ab} , ε_3^{Ab} , and ε_4^{Ab} are vectors of samples of Gaussian functions whose parameters are presented in Table 1.

Table 1. The parameters of the Gaussian functions used for generation of data representative of the residual spectrum.

	ε_1^{Ab}	ε_2^{Ab}	ε_3^{Ab}	ε_4^{Ab}
Mean value	1 700 nm	1 900 nm	2 100 nm	2 400 nm
Standard deviation	8 nm	32 nm	22 nm	15 nm

The low-resolution data $\tilde{\mathbf{y}}^{Tr}$ have been synthesized using Eq.(16) and Eq.(14). The matrix \mathbf{G} has been generated using an empirical apparatus function $g(\lambda)$ shown in Fig. 3. The standard deviation of the noise component has been set to the value $\sigma_\eta = 10^{-3}$, being a typical level of noise in micro-spectrophotometers which are today commercially available.

Fig. 3. The apparatus function $g(\lambda)$ used for experimentation.

The uncertainties of the estimates of concentrations, obtained by means of the compared methods, the BM and the CLSM, have been assessed in a statistical way. Each numerical experiment has been repeated $R = 100$ times, for various realizations of disturbances η and of residual data $\underline{\varepsilon}_r$, and the results $\{\hat{c}_j(r) \mid r = 1, \dots, R\}$ have been used for computing estimates of the relative bias:

$$\hat{b}_j = \frac{1}{R} \sum_{r=1}^R \delta \hat{c}_j(r) \quad \text{for } j = 1, \dots, 3 \quad (33)$$

and of the relative standard deviation:

$$\hat{s}_j = \sqrt{\frac{1}{R-1} \sum_{r=1}^R [\delta \hat{c}_j(r) - \hat{b}_j]^2} \quad \text{for } j = 1, \dots, 3 \quad (34)$$

where:

$$\delta \hat{c}_j(r) = \frac{\hat{c}_j(r) - \dot{c}_j}{\dot{c}_j} \tag{35}$$

6. RESULTS OF INVESTIGATION

The comparison of the BM and the CLSM, based on semi-synthetic data, has been carried out using the two sets of parameters characterizing *a priori* information:

$$\frac{V1 : \bar{c}_1 = \dot{c}_1,}{c_2 = \dot{c}_2 \text{ and } \sigma_v \ni \{10^{-7}, 10^{-6}, 10^{-5}, 10^{-4}, 10^{-3}, 10^{-3}, 10^{-2}, 10^{-1}\}} \tag{36}$$

$$\frac{V2 : \bar{c}_1 = 0.95 \cdot \dot{c}_1,}{c_2 = \dot{c}_2 \text{ and } \sigma_v \ni \{10^{-7}, 10^{-6}, 10^{-5}, 10^{-4}, 10^{-3}, 10^{-3}, 10^{-2}, 10^{-1}\}} \tag{37}$$

where \dot{c}_1 and \dot{c}_2 are the exact values of concentrations used for the data synthesis. In both cases, the value of level has been set to 10^{-3} . The results of computation, obtained for $M = N = 501$, are presented in Figs 4–9 using the following types of lines to differentiate the results corresponding to the three concentrations:

$$c_1 \text{ ——— } c_2 \text{ } \circ \text{---} \circ \text{---} \circ \text{---} c_3 \text{ - - - -}$$

The lines representative of the results obtained by means of the BM are black, and the lines representative of the results obtained by means of the CLSM are red. For the sake of editorial space economy, only selected results are presented in the graphical form. More complete numerical results of computation are shown in Tables 1-4 containing the maximum values of $b\hat{j}$ and $s\hat{j}$, obtained for both compared methods: the BM and the CLSM.

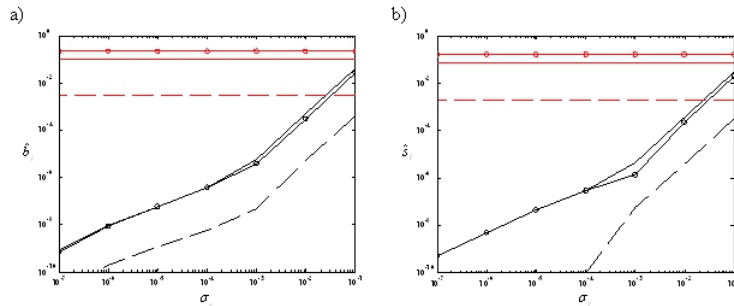


Fig. 4. The results obtained for $\dot{c}_1 = 0.01$, $\dot{c}_2 = 0.01$, and the V1 version of *a priori* information.

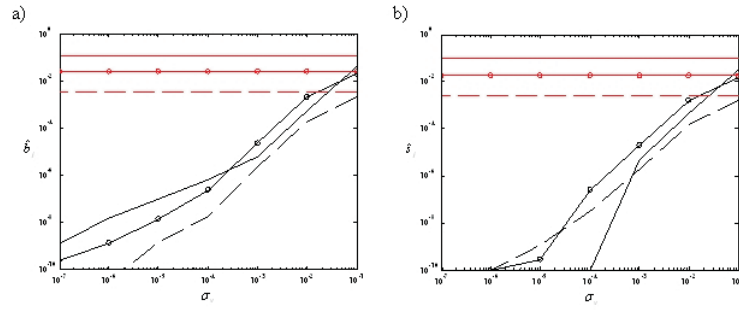


Fig. 5. The results obtained for $c_1 = 0.01$, $c_2 = 0.09$, and the V1 version of *a priori* information.

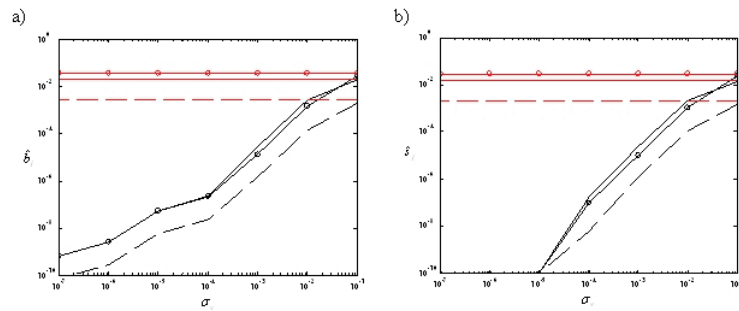


Fig. 6. The results obtained for $c_1 = 0.05$, $c_2 = 0.05$, and the V1 version of *a priori* information.

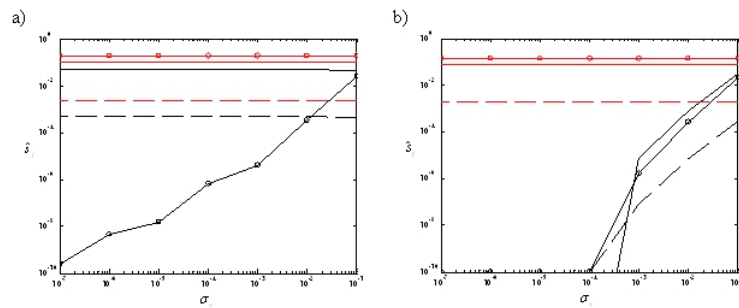


Fig. 7. The results obtained for $c_1 = 0.01$, $c_2 = 0.01$, and the V2 version of *a priori* information.

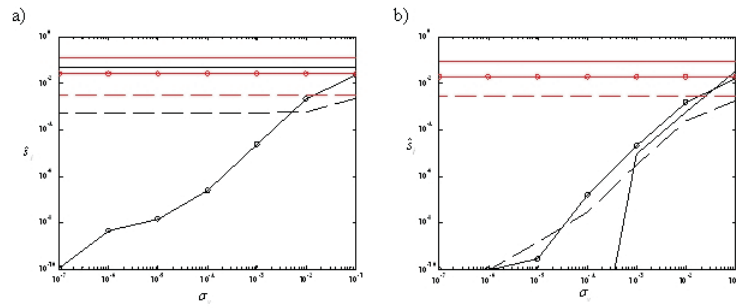


Fig. 8. The results obtained for $c_1 = 0.01$, $c_2 = 0.09$, and the V2 version of *a priori* information.

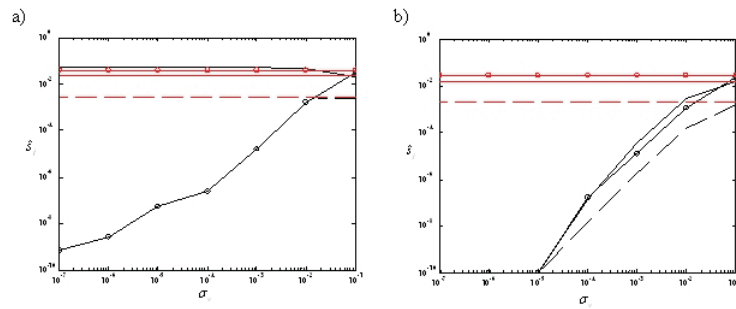


Fig. 9. The results obtained for $c_1 = 0.05$, $c_2 = 0.05$, and the V2 version of *a priori* information.

Table 1. The maximum values of \hat{b}_j , obtained for the V1 version of *a priori* information (in brackets: the indices of concentrations corresponding to those values).

		BM							CLSM
		σ_v							
\hat{c}_1	\hat{c}_2	10^{-7}	10^{-6}	10^{-5}	10^{-4}	10^{-3}	10^{-2}	10^{-1}	
0.01	0.01	$8.07 \cdot 10^{-10}$ (1)	$9.46 \cdot 10^{-9}$ (1)	$5.76 \cdot 10^{-8}$ (1)	$3.93 \cdot 10^{-7}$ (1)	$5.81 \cdot 10^{-6}$ (1)	$5.15 \cdot 10^{-4}$ (1)	$4.18 \cdot 10^{-2}$ (1)	$2.22 \cdot 10^{-1}$ (2)
0.01	0.05	$1.31 \cdot 10^{-9}$ (1)	$1.41 \cdot 10^{-8}$ (1)	$1.01 \cdot 10^{-7}$ (1)	$6.74 \cdot 10^{-7}$ (1)	$1.42 \cdot 10^{-5}$ (2)	$1.45 \cdot 10^{-3}$ (2)	$3.98 \cdot 10^{-2}$ (1)	$1.14 \cdot 10^{-1}$ (1)
0.01	0.09	$1.31 \cdot 10^{-9}$ (1)	$1.46 \cdot 10^{-8}$ (1)	$1.01 \cdot 10^{-7}$ (1)	$6.74 \cdot 10^{-7}$ (1)	$2.39 \cdot 10^{-5}$ (2)	$2.07 \cdot 10^{-3}$ (2)	$4.10 \cdot 10^{-2}$ (1)	$1.23 \cdot 10^{-1}$ (1)
0.05	0.01	$1.31 \cdot 10^{-9}$ (2)	$1.41 \cdot 10^{-8}$ (2)	$1.01 \cdot 10^{-7}$ (2)	$6.74 \cdot 10^{-7}$ (2)	$2.58 \cdot 10^{-5}$ (1)	$2.26 \cdot 10^{-3}$ (1)	$2.37 \cdot 10^{-2}$ (2)	$2.01 \cdot 10^{-1}$ (2)
0.05	0.05	$6.69 \cdot 10^{-10}$ (1)	$2.58 \cdot 10^{-9}$ (1)	$5.42 \cdot 10^{-8}$ (1)	$2.38 \cdot 10^{-7}$ (1)	$2.82 \cdot 10^{-5}$ (1)	$2.82 \cdot 10^{-3}$ (1)	$3.00 \cdot 10^{-2}$ (2)	$3.90 \cdot 10^{-2}$ (2)
0.05	0.09	$6.69 \cdot 10^{-10}$ (1)	$4.49 \cdot 10^{-9}$ (2)	$5.42 \cdot 10^{-8}$ (1)	$3.11 \cdot 10^{-7}$ (1)	$2.61 \cdot 10^{-5}$ (1)	$2.51 \cdot 10^{-3}$ (1)	$2.34 \cdot 10^{-2}$ (2)	$2.54 \cdot 10^{-2}$ (2)
0.09	0.01	$1.31 \cdot 10^{-9}$ (2)	$1.46 \cdot 10^{-8}$ (2)	$1.01 \cdot 10^{-7}$ (2)	$6.74 \cdot 10^{-7}$ (2)	$4.72 \cdot 10^{-5}$ (1)	$3.16 \cdot 10^{-3}$ (1)	$2.54 \cdot 10^{-2}$ (2)	$2.24 \cdot 10^{-1}$ (2)
0.09	0.05	$6.69 \cdot 10^{-10}$ (2)	$4.49 \cdot 10^{-9}$ (1)	$5.42 \cdot 10^{-8}$ (2)	$4.43 \cdot 10^{-7}$ (1)	$5.21 \cdot 10^{-5}$ (1)	$3.26 \cdot 10^{-3}$ (1)	$2.97 \cdot 10^{-2}$ (2)	$4.02 \cdot 10^{-2}$ (2)
0.09	0.09	$7.75 \cdot 10^{-10}$ (1)	$1.03 \cdot 10^{-8}$ (2)	$6.63 \cdot 10^{-8}$ (2)	$5.53 \cdot 10^{-7}$ (1)	$4.87 \cdot 10^{-5}$ (1)	$3.77 \cdot 10^{-3}$ (1)	$2.03 \cdot 10^{-2}$ (2)	$2.11 \cdot 10^{-2}$ (2)

Table 2. The maximum values of $\hat{\epsilon}_j$, obtained for the V1 version of *a priori* information (in brackets: the indices of concentrations corresponding to those values).

		BM							CLSM
		σ_v							
\hat{c}_1	\hat{c}_1	10^{-7}	10^{-6}	10^{-5}	10^{-4}	10^{-3}	10^{-2}	10^{-1}	
0.01	0.01	$5.33 \cdot 10^{-10}$ (1)	$4.80 \cdot 10^{-9}$ (1)	$4.32 \cdot 10^{-8}$ (1)	$2.88 \cdot 10^{-7}$ (1)	$4.55 \cdot 10^{-6}$ (1)	$3.94 \cdot 10^{-4}$ (1)	$3.42 \cdot 10^{-2}$ (1)	$1.65 \cdot 10^{-1}$ (2)
0.01	0.05	0	0	0	$2.31 \cdot 10^{-8}$ (2)	$1.16 \cdot 10^{-5}$ (2)	$1.04 \cdot 10^{-3}$ (2)	$3.53 \cdot 10^{-2}$ (1)	$8.65 \cdot 10^{-2}$ (1)
0.01	0.09	0	0	$1.15 \cdot 10^{-9}$ (3)	$2.61 \cdot 10^{-7}$ (2)	$1.96 \cdot 10^{-5}$ (2)	$1.57 \cdot 10^{-3}$ (2)	$3.39 \cdot 10^{-2}$ (1)	$9.49 \cdot 10^{-2}$ (1)
0.05	0.01	0	0	0	$1.83 \cdot 10^{-7}$ (1)	$1.97 \cdot 10^{-5}$ (1)	$1.64 \cdot 10^{-3}$ (1)	$1.94 \cdot 10^{-2}$ (2)	$1.53 \cdot 10^{-1}$ (2)
0.05	0.05	0	0	0	$1.67 \cdot 10^{-7}$ (1)	$2.28 \cdot 10^{-5}$ (1)	$2.05 \cdot 10^{-3}$ (1)	$2.45 \cdot 10^{-2}$ (2)	$2.88 \cdot 10^{-2}$ (2)
0.05	0.09	0	0	0	$3.09 \cdot 10^{-7}$ (1)	$1.96 \cdot 10^{-5}$ (1)	$1.88 \cdot 10^{-3}$ (1)	$1.70 \cdot 10^{-2}$ (1)	$2.00 \cdot 10^{-2}$ (2)
0.09	0.01	0	0	$1.13 \cdot 10^{-9}$ (3)	$3.67 \cdot 10^{-7}$ (1)	$3.63 \cdot 10^{-5}$ (1)	$2.37 \cdot 10^{-3}$ (1)	$2.34 \cdot 10^{-2}$ (2)	$1.56 \cdot 10^{-1}$ (2)
0.09	0.05	0	0	0	$4.21 \cdot 10^{-7}$ (1)	$3.83 \cdot 10^{-5}$ (1)	$2.31 \cdot 10^{-3}$ (1)	$2.20 \cdot 10^{-2}$ (2)	$3.18 \cdot 10^{-2}$ (2)
0.09	0.09	$5.34 \cdot 10^{-10}$ (1)	$4.69 \cdot 10^{-9}$ (1)	$4.24 \cdot 10^{-8}$ (1)	$3.57 \cdot 10^{-7}$ (1)	$3.94 \cdot 10^{-5}$ (1)	$2.64 \cdot 10^{-3}$ (1)	$1.54 \cdot 10^{-2}$ (2)	$1.55 \cdot 10^{-2}$ (2)

Table 3. The maximum values of \hat{b}_j , obtained for the V2 version of *a priori* information (in brackets: the indices of concentrations corresponding to those values).

		BM							CLSM
		σ_v							
\hat{c}_1	\hat{c}_1	10^{-7}	10^{-6}	10^{-5}	10^{-4}	10^{-3}	10^{-2}	10^{-1}	
0.01	0.01	$5.00 \cdot 10^{-2}$ (1)	$4.98 \cdot 10^{-2}$ (1)	$4.34 \cdot 10^{-2}$ (1)	$1.97 \cdot 10^{-1}$ (2)				
0.01	0.05	$5.00 \cdot 10^{-2}$ (1)	$4.97 \cdot 10^{-2}$ (1)	$4.64 \cdot 10^{-2}$ (1)	$1.04 \cdot 10^{-1}$ (1)				
0.01	0.09	$5.00 \cdot 10^{-2}$ (1)	$4.98 \cdot 10^{-2}$ (1)	$5.14 \cdot 10^{-2}$ (1)	$1.22 \cdot 10^{-1}$ (1)				
0.05	0.01	$5.00 \cdot 10^{-2}$ (1)	$4.99 \cdot 10^{-2}$ (1)	$4.43 \cdot 10^{-2}$ (1)	$2.65 \cdot 10^{-2}$ (2)	$2.40 \cdot 10^{-1}$ (2)			
0.05	0.05	$5.00 \cdot 10^{-2}$ (1)	$4.99 \cdot 10^{-2}$ (1)	$4.50 \cdot 10^{-2}$ (1)	$3.16 \cdot 10^{-2}$ (2)	$3.90 \cdot 10^{-2}$ (2)			
0.05	0.09	$5.00 \cdot 10^{-2}$ (1)	$4.99 \cdot 10^{-2}$ (1)	$4.44 \cdot 10^{-2}$ (1)	$1.95 \cdot 10^{-2}$ (2)	$2.32 \cdot 10^{-2}$ (1)			
0.09	0.01	$5.00 \cdot 10^{-2}$ (1)	$4.98 \cdot 10^{-2}$ (1)	$3.73 \cdot 10^{-2}$ (1)	$2.53 \cdot 10^{-2}$ (2)	$2.14 \cdot 10^{-1}$ (2)			
0.09	0.05	$5.00 \cdot 10^{-2}$ (1)	$4.98 \cdot 10^{-2}$ (1)	$3.76 \cdot 10^{-2}$ (1)	$3.42 \cdot 10^{-2}$ (2)	$3.92 \cdot 10^{-2}$ (2)			
0.09	0.09	$5.00 \cdot 10^{-2}$ (1)	$4.98 \cdot 10^{-2}$ (1)	$3.76 \cdot 10^{-2}$ (1)	$1.88 \cdot 10^{-2}$ (2)	$2.32 \cdot 10^{-2}$ (2)			

Table 4. The maximum values of $\hat{\delta}_j$, obtained for the V2 version of *a priori* information (in brackets: the indices of concentrations corresponding to those values).

		BM							CLSM
		σ_v							
\hat{c}_1	\hat{c}_1	10^{-7}	10^{-6}	10^{-5}	10^{-4}	10^{-3}	10^{-2}	10^{-1}	
0.01	0.01	0	$1.31 \cdot 10^{-16}$ (1)	$1.20 \cdot 10^{-16}$ (1)	$1.20 \cdot 10^{-16}$ (1)	$7.17 \cdot 10^{-6}$ (1)	$7.54 \cdot 10^{-4}$ (1)	$3.22 \cdot 10^{-2}$ (1)	$1.39 \cdot 10^{-1}$ (2)
0.01	0.05	0	$1.31 \cdot 10^{-16}$ (1)	$1.20 \cdot 10^{-16}$ (1)	$2.30 \cdot 10^{-8}$ (2)	$1.08 \cdot 10^{-5}$ (2)	$1.04 \cdot 10^{-3}$ (2)	$3.53 \cdot 10^{-2}$ (1)	$7.71 \cdot 10^{-2}$ (1)
0.01	0.09	0	$1.31 \cdot 10^{-16}$ (1)	$1.43 \cdot 10^{-9}$ (3)	$1.61 \cdot 10^{-7}$ (2)	$1.96 \cdot 10^{-5}$ (2)	$1.50 \cdot 10^{-3}$ (2)	$3.23 \cdot 10^{-2}$ (1)	$9.45 \cdot 10^{-2}$ (1)
0.05	0.01	$1.05 \cdot 10^{-16}$ (1)	$1.31 \cdot 10^{-16}$ (1)	$1.05 \cdot 10^{-16}$ (1)	$3.27 \cdot 10^{-7}$ (1)	$3.14 \cdot 10^{-5}$ (1)	$2.91 \cdot 10^{-3}$ (1)	$2.06 \cdot 10^{-2}$ (2)	$1.68 \cdot 10^{-1}$ (2)
0.05	0.05	$1.05 \cdot 10^{-16}$ (1)	$1.31 \cdot 10^{-16}$ (1)	0	$1.67 \cdot 10^{-7}$ (2)	$3.39 \cdot 10^{-5}$ (1)	$2.96 \cdot 10^{-3}$ (1)	$2.41 \cdot 10^{-2}$ (2)	$2.88 \cdot 10^{-2}$ (2)
0.05	0.09	$1.05 \cdot 10^{-16}$ (1)	$1.31 \cdot 10^{-16}$ (1)	0	$2.79 \cdot 10^{-7}$ (1)	$3.57 \cdot 10^{-5}$ (1)	$2.71 \cdot 10^{-3}$ (1)	$1.45 \cdot 10^{-2}$ (1)	$1.84 \cdot 10^{-2}$ (1)
0.09	0.01	$3.54 \cdot 10^{-11}$ (1)	$1.16 \cdot 10^{-16}$ (1)	$4.04 \cdot 10^{-9}$ (1)	$5.18 \cdot 10^{-7}$ (1)	$5.42 \cdot 10^{-5}$ (1)	$3.90 \cdot 10^{-3}$ (1)	$2.32 \cdot 10^{-2}$ (2)	$1.66 \cdot 10^{-1}$ (2)
0.09	0.05	$1.36 \cdot 10^{-16}$ (1)	$1.16 \cdot 10^{-16}$ (1)	$8.60 \cdot 10^{-9}$ (1)	$5.90 \cdot 10^{-7}$ (1)	$5.18 \cdot 10^{-5}$ (1)	$3.26 \cdot 10^{-3}$ (1)	$2.40 \cdot 10^{-2}$ (2)	$2.72 \cdot 10^{-2}$ (2)
0.09	0.09	$3.34 \cdot 10^{-10}$ (1)	$1.16 \cdot 10^{-16}$ (1)	0	$4.43 \cdot 10^{-7}$ (2)	$5.37 \cdot 10^{-5}$ (1)	$3.83 \cdot 10^{-3}$ (1)	$1.33 \cdot 10^{-2}$ (2)	$1.78 \cdot 10^{-2}$ (2)

7. DISCUSSION AND CONCLUSIONS

The comparison of the BM with the CLSM, based on the criteria related to measurement uncertainty, has been essentially aimed at the assessment of the robustness of these methods to four influencing factors:

- systematic distortion of spectral data by the limited optical resolution of the ST, characterised by the apparatus function $g(\lambda)$;
- random uncorrelated disturbances in the spectral data, characterized by the standard deviation σ_v ;

- random correlated disturbances in the spectral data, modelling residual spectra of components not identified in the analysis, and characterized by the parameter *level*;
- imprecision of a priori information on the estimated concentrations, characterized by the variance σ_v .

The overview of the results, presented in Figures 4–9 and in Tables 1–4, enables one to notice their consistence:

- The values of uncertainty indicators, obtained for \hat{c}_1 and \hat{c}_2 , are comparable.
- If $\sigma_v = 10^{-7}$, the estimation uncertainty, both the relative bias and the relative standard deviation, is for the BM by several orders of magnitude lower than for the CLSM.

– The estimation uncertainty for the BM is growing with σ_v and it is approaching that of the CLSM when σ_v is approaching $\sigma_v = 10^{-1}$.

Taking into account that the interval of a priori expanded uncertainty, corresponding to the latter value is comparable with ca. 50 % of the range of the measurand variability, one may conclude that this is a very positive feature of the BM. Both uncertainty indicators, the relative bias and the relative standard deviation, are equally important because their corresponding values are – as a rule – of the same order of magnitude. The results obtained demonstrate the significant superiority of the BM over the CLSM both in terms of the relative bias and in terms of the relative standard deviation. These results show also the importance of a priori information on the solution for the performance of the BM. As shown in Figures 7–9, the detuning of the parameter $\frac{1}{c_1}$ from \hat{c}_1 by $\pm 5\%$ has implied the increase of the relative bias of the estimates to a level slightly lower than that of the bias generated by the CLSM – without affecting their relative standard deviation. Taking into account that the expanded uncertainty is composed of the bias and a multiplicity of the standard deviation, one may conclude that for a variation of concentrations limited to $\pm 5\%$ of their typical values, the BM may provide significantly more accurate estimates than the CLSM.

The results obtained demonstrate a significant potential behind the BM to enhance the effectiveness of the application of low-resolution spectrophotometers for solving monitoring-type problems that appear in food manufacturing associated with oil mixing. As a rule, in this type of problems, a considerable amount of statistical information on the variation of the monitored concentrations is available and may be used as *a priori* information for the BM. The gains in accuracy of estimation depend on the precision of this information; evidently, false information is worse than its absence.

ACKNOWLEDGEMENTS

The study presented in this paper is supported by the Ministry of Science and Higher Education in Poland (grant No. N505 011 31/1428). The authors express their sincere gratitude to Dr. Grażyna Zofia Żukowska from the Faculty of Chemistry, Warsaw University of Technology, for the acquisition of data used in the paper for numerical experimentation.

REFERENCES

1. Tay A., Singh R. K., Krishnan S. S., Gore J. P.: "Authentication of Olive Oil Adulterated with Vegetable Oils Using Fourier Transform Infrared Spectroscopy", *Lebensm.-Wiss. u.-Technol.*, vol. 35, 2002, pp. 99–103.
2. Christy A., Kasemusumran S., Du Y., Ozaki Y.: "The Detection and Quantification of Adulteration in Olive oil by Near-Infrared Spectroscopy and Chemometrics", *Anal. Sci.*, vol. 20, June 2004, pp. 935–940.
3. Armenta S., Garrigues S., de la Guardia M.: "Determination of Edible Oil Parameters by Near Infrared Spectrometry", *Anal. Chim. Acta*, vol. 596, 2007, pp. 330–337.
4. Özdemir D., Öztürk B.: "Near Infrared Spectroscopic Determination of Olive Oil Adulteration with Sunflower and Corn Oil", *J. Food & Drug Anal.*, vol. 15, no. 1, 2007, pp. 40–47.
5. Sinelli N., Casiraghi E., Tura D., Downey G.: "Characterization and Classification of Italian Virgin Olive Oils by Near and Medium Infrared Spectroscopy", *Proc. 13th Int. Conf. Near Infrared Spectroscopy* (Umeå-Vasa, Sweden & Finland, June 15–21, 2007, paper 4–6.
6. Niedziński C.: *Bayesian Method for Estimation of Concentrations in Spectrophotometric Analysis of Multicomponent Substances*, Ph.D. Thesis completed at the Faculty of Electronics and Information Technology, Warsaw University of Technology (advisor: R. Z. Morawski), December 2007 (in Polish).
7. Wiśniewski M., Morawski R. Z., Barwicz A.: "Modeling the Spectrometric Microtransducer", *IEEE T. Instrum. Meas.*, June 1999, vol. 48, no. 3, pp. 747–752.
8. Leonard T., Hsu J. S. J.: *Bayesian Methods*. Cambridge University Press 1999.
9. <http://tomopt.com/tomlab/> [as of July 2008].

Appendix: List of mathematical symbols

A	– a normalization factor of the <i>a priori</i> probability distribution of the random vector \underline{c} ;
\arg_v	– the operator “solving” the equation or optimization problem, whose description follows, with respect to a variable v ;
α_n	– a vector of parameters of the “static” characteristic of the ST;
b_j	– the relative bias of the estimator of the concentration c_j , $j = 1, \dots, J$; \hat{b}_j – its estimate;
\hat{c}_j	– the exact value of the concentration c_j ;
\mathbf{c}	– vector of the concentrations of J components of a substance to be analyzed (<i>i.e.</i> of an analyte); $\mathbf{c} = [c_1 \dots c_J]^T$;
\underline{c}	– the randomized vector of the concentrations; $\underline{c} = [\underline{c}_1 \dots \underline{c}_J]^T$;
$\bar{\mathbf{c}}$	– a vector parameter controlling the mean value of the <i>a priori</i> probability distribution of the random vector \underline{c}
C	– et of constraints the vector of concentrations is subject to;
$\text{CAT}[\bullet]$	– the operator of absorbance-to-transmittance transformation;
$\delta \hat{c}_j$	– the relative error of the estimate \hat{c}_j of the concentration c_j ; $\delta \hat{c}_j = (\hat{c}_j - c_j)/c_j$;
$\text{E}[\bullet]$	– the operator of “computing” the mean value of a random variable or random vector;
$\underline{\varepsilon}$	– the random vector modelling samples of the residual spectrum corresponding to unexpected or neglected components; $= [\underline{\varepsilon}_1 \dots \underline{\varepsilon}_M]^T$;
$f_c(\mathbf{c})$	– the <i>a priori</i> probability density function for \mathbf{c} , the so-called prior;
$f_{\tilde{\mathbf{y}}^{Tr}}(\tilde{\mathbf{y}}^{Tr})$	– the <i>a priori</i> probability density function for $\tilde{\mathbf{y}}^{Tr}$;
$f_{\underline{c} \tilde{\mathbf{y}}^{Tr}}(\underline{c} \tilde{\mathbf{y}}^{Tr})$	– the <i>a posteriori</i> probability density function for \underline{c} conditional on $\tilde{\mathbf{y}}^{Tr}$ the so-called posterior;
$f_{\tilde{\mathbf{y}}^{Tr} \underline{c}}(\tilde{\mathbf{y}}^{Tr} \underline{c})$	– the probability density function for $\tilde{\mathbf{y}}^{Tr}$ conditional on \underline{c} ; the so-called likelihood;
$F(\hat{y}_n; \alpha_n)$	– the inverse “static” characteristic of the ST;
$g_n(\lambda)$	– the response of the optical part of the ST to a monochromatic optical signal observed at the n th output of the ST;
$\underline{\eta}$	– the randomized vector of additive residuals representing the total uncertainty of data modelling; $\underline{\eta} = [\eta_1 \dots \eta_N]^T$;
$\inf\{\bullet\}$	– the operator “computing” the infimum of the sequence or function in brackets $\{\bullet\}$;
J	– the number of the components of the analyte;
<i>level</i>	– an indicator of the level of the residual spectrum;
λ	– the wavelength;
$\lambda_{\min}, \lambda_{\max}$	– the minimum and maximum wavelength values limiting the wavelength range of the ST;
$\{\lambda'_m\}$	– the sequence of wavelength values corresponding to the spectrum sampling within the numerical algorithms; $\{\lambda'_m\} \equiv \{\lambda'_m m = 1, \dots, M\}$;
$\{\lambda_n\}$	– a sequence of wavelength values corresponding to the data at the ST output; $\{\lambda_n\} \equiv \{\lambda_n n = 1, \dots, N\}$;
M	– the number of samples the spectrum is represented within the numerical algorithms;
N	– the number of raw data provided by the ST;
$\underline{\mu}_c$	– the mean value of the random vector \underline{c} ; $\underline{\mu}_c = \text{E}[\underline{c}]$;
$\underline{\mu}_\varepsilon$	– the mean value of the random vector $\underline{\varepsilon}$; $\underline{\mu}_\varepsilon = \text{E}[\underline{\varepsilon}]$;
R	– the number of repetitions of each numerical experiment;
s_j	– the relative standard deviation of the estimator of the concentration c_j , $j = 1, \dots, J$; \hat{s}_j – its estimate;
$\sup\{\bullet\}$	– the operator “computing” the supremum of the sequence or function in brackets $\{\bullet\}$;
σ_c	– the standard deviation of an element or of the j th element of the random vector \underline{c} , $j = 1, \dots, J$;

- σ_v – a scalar parameter controlling the standard deviation of the *a priori* probability distribution of the random vector c ;
- σ_η – the standard deviation of an element of the vector η ;
- $\mathbf{v}(\mathbf{c})$ – a $(J - 1)$ dimensional vector whose elements are defined by the rational transformation of the finite interval into the infinite interval $(-\infty; +\infty)$;
- $x(\lambda)$ – the intensity spectrum of the ST input optical signal;
- $x^{Ab}(\lambda)$ – the absorbance spectrum of the analyte;
- $x_j^{Ab}(\lambda)$ – the normalized spectrum of the j th component of the analyte; $j = 1, \dots, J$;
- $x^{Tr}(\lambda)$ – the transmittance spectrum of the analyte;
- \mathbf{x}_j^{Ab} – the vector containing M equidistant samples of the spectrum
 $x_j^{Ab}(\lambda), j = 1, \dots, J; \mathbf{x}_j^{Ab} = [x_j^{Ab}(\lambda'_1) \dots x_j^{Ab}(\lambda'_M)]^T$;
- \mathbf{x}^{Tr} – the vector containing M equidistant samples of the transmittance spectrum $x(\lambda)$;
 $\mathbf{x}^{Tr} = [x^{Tr}(\lambda'_1) \dots x^{Tr}(\lambda'_M)]^T$;
- \mathbf{X}^{Ab} – the matrix composed of the vectors $\mathbf{x}_j^{Ab}, j = 1, \dots, J; \mathbf{X}^{Ab} = [\mathbf{x}_1^{Ab} \dots \mathbf{x}_J^{Ab}]$;
- $\tilde{\mathbf{y}}$ – the raw intensity-domain data; $\tilde{\mathbf{y}} = [\tilde{y}_1 \dots \tilde{y}_N]^T$;
- $\hat{\mathbf{y}}$ – an estimate of the raw data $\tilde{\mathbf{y}}$ generated by the mathematical model of those data;
 $\hat{\mathbf{y}} = [\hat{y}_1 \dots \hat{y}_N]^T$;
- $\tilde{\mathbf{y}}^{Ab}$ – the raw absorbance-domain data; $\tilde{\mathbf{y}}^{Ab} = [\tilde{y}_1^{Ab} \dots \tilde{y}_N^{Ab}]^T$;
- $\tilde{\mathbf{y}}^{Tr}$ – the raw transmittance-domain data; $\tilde{\mathbf{y}}^{Tr} = [\tilde{y}_1^{Tr} \dots \tilde{y}_N^{Tr}]^T$.